Moderate L-lactate administration suppresses adipose tissue macrophage M1 polarization to alleviate obesity-associated insulin resistance

Hao Cai[1], **Xin Wang**[1], **Zhixin Zhang**[1], **Juan Chen**[1], **Fangbin Wang**[1], **Lu Wang**[1], and **Jian Liu**[1,2,*]

From the [1]*School of Food and Biological Engineering, and* [2]*Engineering Research Center of Bioprocess, Ministry of Education, Hefei University of Technology, Hefei, Anhui, China*

Edited by Qi Qun Tang

As a crucial metabolic intermediate, L-lactate is involved in redox balance, energy balance, and acid–base balance in organisms. Moderate exercise training transiently elevates plasma L-lactate levels and ameliorates obesity-associated type 2 diabetes. However, whether moderate L-lactate administration improves obesity-associated insulin resistance remains unclear. In this study, we defined 800 mg/kg/day as the dose of moderate L-lactate administration. In mice fed with a high-fat diet (HFD), moderate L-lactate administration for 12 weeks was shown to alleviate weight gain, fat accumulation, and insulin resistance. Along with the phenotype alterations, white adipose tissue thermogenesis was also found to be elevated in HFD-fed mice. Meanwhile, moderate L-lactate administration suppressed the infiltration and proinflammatory M1 polarization of adipose tissue macrophages (ATMs) in HFD-fed mice. Furthermore, L-lactate treatment suppressed the lipopolysaccharide-induced M1 polarization of bone marrow–derived macrophages (BMDMs). L-lactate can bind to the surface receptor GPR132, which typically drives the downstream cAMP–PKA signaling. As a nutrient sensor, AMP-activated protein kinase (AMPK) critically controls macrophage inflammatory signaling and phenotype. Thus, utilizing inhibitors of the kinases PKA and AMPK as well as siRNA against GPR132, we demonstrated that GPR132–PKA–AMPKα1 signaling mediated the suppression caused by L-lactate treatment on BMDM M1 polarization. Finally, L-lactate addition remarkably resisted the impairment of lipopolysaccharide-treated BMDM conditional media on adipocyte insulin sensitivity. In summary, moderate L-lactate administration suppresses ATM proinflammatory M1 polarization through activation of the GPR132–PKA–AMPKα1 signaling pathway to improve insulin resistance in HFD-fed mice, suggesting a new therapeutic and interventional approach to obesity-associated type 2 diabetes.

Mammalian cells and tissues execute their metabolic tasks through exchanging energy metabolites from the circulatory system, in which glucose and L-lactate are the major caloric carriers (1, 2). L-lactate is the dominant isomeric form compared with D-lactate in mammals and is mainly derived from glucose *via* glycolysis. Circulating L-lactate travels among the organs, cells, and organelles as an oxidative and gluconeogenic substrate, which is defined as "lactate shuttle," and plays a critical role in preserving redox balance, energy balance, and acid–base balance (2). In normal physiological conditions of humans and rodents, the plasma L-lactate concentration is at 0.5 to 2 mM (2, 3). When the circulating L-lactate level exceeds the basal range, it may negatively or positively affect the health of the organism. On the one hand, the local L-lactate level is up to 40 mM in the malignant tumor microenvironment because of aerobic glycolysis, and the plasma L-lactate concentrations also persist higher levels than those in normal physiological conditions (4, 5). In some tumors, such as non–small-cell lung carcinoma and cutaneous squamous cell carcinoma, the higher local L-lactate levels help tumor cells evade the surveillance of T cells and natural killer cells and hence accelerate the tumorigenesis (6). On the other hand, it is widely known that moderate exercise has beneficial effects on the metabolic health of the organism (7). The plasma L-lactate concentration is approximately increased to 4 mM during moderate exercise training and rapidly returns to normal physiological level in 1 to 3 h after exercise training (2, 8). The transient increment of L-lactate concentration protects muscle from injury by delivering a neural signal that produces pain to reduce exercise intensity, rather than causing muscle fatigue (9, 10). Recent studies by Takahashi *et al.* (11) further indicated that exercise-induced L-lactate could promote the secretion of adipokine transforming growth factor β2 (TGF-β2), which improved glucose homeostasis in the mice fed with a high-fat diet (HFD). Thus, the moderate elevation of plasma L-lactate concentration may positively affect the health of the organism. It deserves to explore whether exogenous moderate L-lactate administration could ameliorate diet-induced obesity and associated insulin resistance.

Obesity and associated insulin resistance are essentially because of persistent caloric absorption exceeding caloric expenditure. Therapeutic targeting of brown adipocyte–mediated thermogenesis to increase caloric expenditure has been regarded as a viable approach to combat obesity and associated insulin resistance (12). In addition, excess nutrition

* For correspondence: Jian Liu, liujian509@hfut.edu.cn.

absorption results in adipocyte hypertrophy and adipose tissue inflammation during the development of diet-induced obesity (13, 14). Meanwhile, the proportions of multiple immune cell populations are altered in adipose tissues, and adipose tissue macrophages (ATMs) are regarded as the primary contributors to adipose tissue inflammation and systemic insulin resistance (14, 15). Compared with those of lean individuals, obese adipose tissues have an increased proportion of total macrophages and a decreased ratio of the M2-like anti-inflammatory macrophages to the M1-like proinflammatory macrophages, which exacerbates local and systemic insulin resistance (15). Conversely, a series of endogenous molecules have been reported to modify the M1/M2 ratio of ATMs and reverse insulin resistance in obese individuals (11, 16–20). For instance, several cytokines, such as interleukin 4 (IL-4), IL-13, and TGF-β2 (11, 16), were shown to suppress ATM M1 polarization and improve adipose tissue inflammation. Some neurotransmitters, such as catecholamine and ceramide (17, 18), were suggested to restrict the proinflammatory polarization of ATMs and the synthesis of inflammatory cytokines. Recently, two energy metabolites, glutamine and succinate (19, 20), were found to participate in mitochondrial metabolism and boost the secretion of type 2 cytokines in ATMs. However, the functional correlation between L-lactate treatment and ATM polarization in the development of obesity-associated insulin resistance remains unclear.

Among multiple signals regulating energy metabolism homeostasis, AMP-activated protein kinase (AMPK) is a master sensor of glucose uptake, fatty acid oxidation, and mitochondrial biogenesis (21). In addition, AMPK is a critical molecule that suppresses macrophage inflammatory signals and transforms macrophages into an anti-inflammatory phenotype (22–24). As a catalytic subunit of AMPK, the activation of AMPKα1 inhibits several inflammatory transcription factors and ultimately reduces the secretion of proinflammatory cytokines, such as tumor necrosis factor alpha (TNF-α), monocyte chemoattractant protein 1 (MCP-1), IL-1β, and interferon gamma (25, 26). Moreover, AMPKα1 could be activated by L-lactate, participating in mitochondrial uncoupling and lipid deposition in muscle cells and hepatocytes, respectively (27, 28). Therefore, whether L-lactate activates AMPKα1 and relevant signals to suppress macrophage proinflammatory polarization merits further investigation.

In this study, we first affirmed the appropriate dose of moderate L-lactate administration in HFD-fed mice. In the mice fed with either a low-fat diet (LFD) or an HFD, the effects of moderate L-lactate administration for 12 weeks on mouse body weight gain, fat accumulation, and glucose tolerance were examined. Subsequently, we detected the actions of moderate L-lactate administration on adipose tissue thermogenesis, total ATM populations, and ATM subpopulations in the mice. Furthermore, the molecular mechanism of L-lactate affects macrophage M1 polarization, which was explored in bone marrow–derived macrophages (BMDMs). Finally, we identified that L-lactate inhibited proinflammatory M1 polarization in BMDMs and improved associated glucose uptake in 3T3-L1 adipocytes through activating the BMDM AMPKα1 signal.

Results

L-lactate administration reduced diet-induced weight gain in mice

To affirm the dose of moderate L-lactate administration, HFD-fed mice were given with a gradient i.p. injection of L-lactate. L-lactate administration reduced the weight gain in the range of 400 mg/kg/day to 3200 mg/kg/day (Fig. 1A). When the dose was higher than 800 mg/kg/day, the mice sharply lost their weight instead of gaining weight (Fig. 1A). To avoid the acidosis induced by L-lactate overdose injection, we adopted 800 mg/kg/day as the dose of moderate L-lactate administration in the subsequent animal studies. At this dose, the plasma L-lactate concentration was elevated to 6 mM in 0.5 to 1 h after L-lactate injection and returned to the normal physiological level in 3 h (Fig. 1B). Therefore, 5 and 10 mM of L-lactate were used as the treatment concentrations in the subsequent cell studies.

Moderate L-lactate administration ameliorated obesity-associated insulin resistance in mice

The 6-week-old mice were fed on LFD or HFD. To evaluate the effects of moderate L-lactate administration on obesity and associated insulin resistance, the LFD-fed mice or HFD-fed mice were injected with L-lactate solution and named by LL group or HL group. As controls, the other LFD-fed mice or HFD-fed mice were injected with saline and named by LS group or HS group. After 12 weeks, the mice from HS group had higher body weight, fat mass, and serum lipid level than those from LS group (Fig. 1, C–F). Correspondingly, compared with LS group, HS group also had the increased adipocyte size of white adipose tissue (WAT), including epididymal adipose tissue (EAT) and subcutaneous adipose tissue (SAT) (Fig. 1G). Intriguingly, moderate L-lactate administration resisted these phenotype alterations in HFD-fed mice, although it did not affect body weight gain, fat mass, serum lipid level, and adipocyte size in LFD-fed mice (Fig. 1, C–G).

Obesity is often accompanied by numerous metabolic dysfunctions, especially insulin resistance (13). As expected, the mice from HS group had lower glucose tolerance and insulin tolerance than those from LS group. However, moderate L-lactate administration remarkably alleviated glucose and insulin intolerance in HFD-fed mice (Fig. 1, H and I). During the development of obesity, visceral adipose tissue has greater inflammatory changes than SAT and hence promotes local and systemic insulin resistance (13, 14). In adipocytes with normal insulin sensitivity, insulin stimulation can induce AKT phosphorylation and leads to glucose transporter type 4 (GLUT4) translocation to the plasma membrane and promotes glucose uptake (29, 30). And EAT is a common visceral adipose tissue in mouse studies (13). Thus, in EATs, we examined the mRNA levels of several classical proinflammatory cytokines, including *MCP-1*, *TNF-α*, *IL-1β*, and
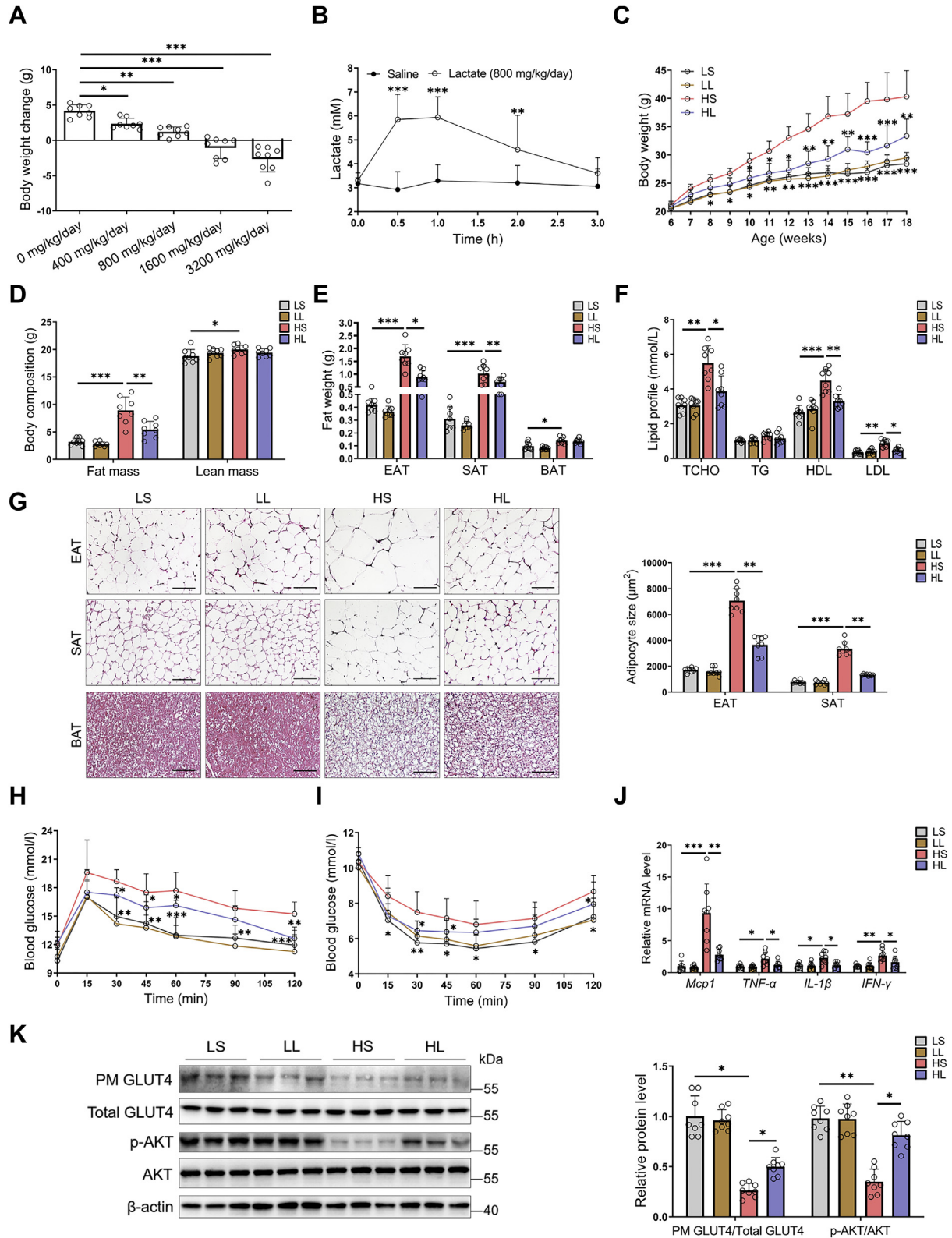
Figure 1. Moderate L-lactate administration ameliorated obesity and associated insulin resistance in mice. At 6 weeks old, HFD-fed male mice were given with a gradient L-lactate injection. *A*, body weight changes after gradient L-lactate injection. *B*, the fluctuations of plasma L-lactate concentration after 800 mg/kg/day injection. In another independent study, 6-week-old male mice were divided into four groups, including LS, LL, HS, and HL groups, and were fed with LFD or HFD for 12 weeks, respectively. *C*, the body weights. *D*, the body composition. *E*, the fat weights. *F*, serum lipid profile. *G*, the adipose tissue H&E staining and adipocyte size; the scale bar represents 100 μm. *H* and *I*, the GTT (*H*) and ITT (*I*). *J*, the mRNA levels of proinflammatory cytokines in EATs. *K*, insulin signaling cascades in EATs in mice without insulin injection. The GLUT4 translocation in EATs and quantification of plasma membrane GLUT4 to total GLUT4; immunoblots for phospho-AKT (Ser-473) and total AKT in EATs and quantification of phosphorylated AKT to total AKT. Data are presented as mean ± SD of eight mice per group, one-way ANOVA with Mann–Whitney test; *$p < 0.05$, **$p < 0.01$, and ***$p < 0.001$. EAT, epididymal adipose tissue; GLUT4, glucose transporter type 4; GTT, glucose tolerance test; HFD, high-fat diet; HS, HFD-saline (i.p.); HL, HFD-lactate (i.p.); ITT, insulin tolerance test; LFD, low-fat diet; LL, LFD-lactate (i.p.); LS, LFD-saline (i.p.); PM, plasma membrane.

Moderate L-lactate administration reduces insulin resistance

interferon gamma, and detected the protein levels of phospho-AKT, AKT, and GLUT4. The mice from HS group have higher expressions of the cytokines (Fig. 1*J*) and lower levels of AKT phosphorylation and GLUT4 translocation (Fig. 1*K*) than those from LS group. Supporting the improvement of moderate L-lactate administration on mouse insulin resistance (Fig. 1, *H* and *I*), the alterations of cytokine level, AKT phosphorylation, and GLUT4 translocation were obviously restored in the mice from HL group (Fig. 1, *J* and *K*). Besides adipose tissues, the expression and activity of insulin signaling molecules were also detected in livers and muscles. In either LFD-fed or HFD-fed mice, moderate L-lactate administration did not alter liver and muscle AKT phosphorylation and liver GLUT2 and muscle GLUT4 translocation (Fig. S1, *A* and *B*). Thus, moderate L-lactate administration ameliorated obesity-associated adipose tissue and systemic insulin resistance in HFD-fed mice.

High plasma L-lactate levels may decrease serum pH value and have a risk of hyperlactatemia or lactic acidosis (31). The hyperlactatemia or lactic acidosis would induce a series of adverse events, such as reduced appetite, hepatosplenomegaly, and hepatic injury (31). Therefore, serum pH value, food and energy intake, liver and spleen weight, liver and spleen morphology, and serum alanine aminotransferase and aspartate transaminase levels were examined in the mice. Of note, there were no differences in serum pH value, food intake, and energy intake among the experimental groups (Fig. S2, *A–C*). In LFD-fed mice, moderate L-lactate administration did not affect liver and spleen weight and their morphologies (Fig. S2, *D–H*). And even in HFD-fed mice, moderate L-lactate administration reversed HFD-induced liver lipid accumulation and serum alanine aminotransferase and aspartate transaminase elevations (Fig. S2, *F–H*). In conclusion, moderate L-lactate administration alleviates obesity-associated insulin resistance, but it does not lead to the development of hyperlactatemia or lactic acidosis.

Moderate L-lactate administration promoted adipose tissue thermogenesis in HFD-fed mice

Persistent imbalance of energy intake and expenditure leads to abnormal body weight gain and metabolic dysfunction (32). Since the mouse energy intake in four groups was comparable (Fig. S2*C*), we evaluated energy expenditure among the groups. Despite there were no differences in O_2 consumption and CO_2 production between the mice from HS group and HL group when the metabolic data were normalized per animal (Fig. S3, *A* and *B*), HL group mice had a higher metabolic rate than HS group mice when the data were normalized to body weight (Fig. S3, *C* and *D*). To determine the short-term effects of moderate L-lactate administration on metabolic rate, we performed a moderate L-lactate injection at 9 AM and 18 PM and detected the metabolic fluctuation during a 24 h light–dark cycle. As expected, when the metabolic data were normalized to body weight, moderate L-lactate administration elevated metabolic rate in HFD-fed mice (Fig. S3, *E* and *F*). Interestingly, compared with LS group, the mice from LL group had an increased metabolic rate within 2 h after moderate L-lactate administration at 9 AM (Fig. S3, *E* and *F*).

And then, we measured the body temperature of four groups of mice. Moderate L-lactate administration turned back HFD-induced body temperature reduction in mice (Fig. 2*A*). In mammals, the maintenance of body temperature needs the involvement of adaptive thermogenesis (12, 32). As two distinct adaptive thermogenic adipocytes, brown and beige adipocytes express uncoupling protein 1 (UCP1) and transform chemical energy into heat energy by the action of UCP1 (12). Thus, we investigated the effect of moderate L-lactate administration on the expressions of some important thermogenic genes, including *Ucp1*, *Pgc-1α*, *Cidea*, and *Prdm16*. Relative to LFD, HFD significantly reduced *Ucp1* expression in WAT, including EAT and SAT (Fig. 2, *B* and *C*). In addition, the mice from LS group had higher WAT *Pgc-1α* and *Cidea* levels than those from HS group (Fig. 2, *B* and *C*). Moderate
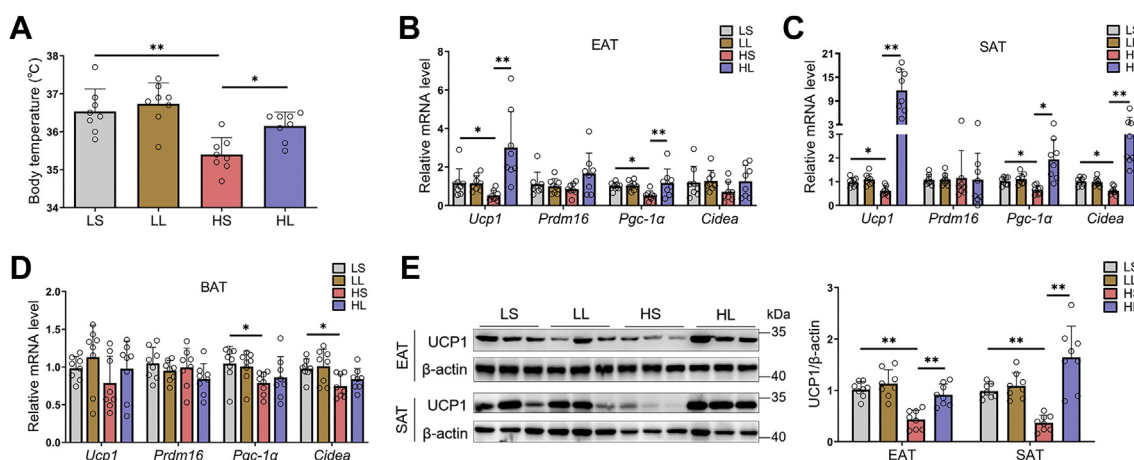

Figure 2. Moderate L-lactate administration promoted adipose tissue thermogenesis in HFD-fed mice. The 6-week-old male mice were divided into four groups, including LS, LL, HS, and HL groups. *A*, the body temperature. *B–D*, the mRNA levels of thermogenic genes in EAT (*B*), SAT (*C*), and BAT (*D*). *E*, immunoblots for UCP1 and the quantification of UCP1 to β-actin in EATs and SATs. Data are presented as mean ± SD of eight mice per group, one-way ANOVA with Mann–Whitney test; *$p < 0.05$, **$p < 0.01$, and ***$p < 0.001$. BAT, brown adipose tissue; EAT, epididymal adipose tissue; HFD, high-fat diet; HL, HFD-lactate (i.p.); HS, HFD-saline (i.p.); LL, LFD-lactate (i.p.); LS, LFD-saline (i.p.); SAT, subcutaneous adipose tissue; UCP1, uncoupling protein 1.

ʟ-lactate administration remarkably elevated WAT thermogenic programs in HFD-fed mice (Fig. 2, *B* and *C*). However, in mouse brown adipose tissue, both HFD and ʟ-lactate administration did not affect *Ucp1* expression (Fig. 2*D*). Supporting the real-time PCR results, immunoblots revealed that moderate ʟ-lactate administration reversed the depression of HFD on WAT UCP1 levels (Fig. 2*E*).

Furthermore, the expressions of genes involved in fatty acid oxidation (*Cpt1a*, *Cpt1b*, *Cpt2*, peroxisome proliferator–activated receptor alpha [*PPARα*], and *Pgc-1α*) and glucose catabolism (*Pkm2* and *G6pc*) were also tested in the livers and skeletal muscles. After moderate ʟ-lactate administration, there were no significant differences in these gene expressions in either LFD-fed or HFD-fed mice (Fig. S4, *A* and *B*). These observations suggest that moderate ʟ-lactate administration promotes WAT thermogenesis. However, given that moderate ʟ-lactate administration did not alter O_2 consumption and CO_2 production in HFD-fed mice when the metabolic data were normalized per animal (Fig. S3, *A* and *B*), whether the improvement of obesity-associated insulin resistance in the mice can be attributed to increased WAT thermogenesis remains in doubt. Therefore, other possible mechanisms affecting adipose tissue and systemic insulin resistance deserve careful investigation.

Moderate ʟ-lactate administration suppressed obesity-induced ATM infiltration and proinflammatory M1 polarization in EATs

In addition to adipocytes, adipose tissue also contains abundant immune cells, in which macrophages have a crucial effect on regulating adipose tissue inflammation and glucose homeostasis in the development of obesity (14). Therefore, we further focused on the impacts of moderate ʟ-lactate administration on ATM infiltration and polarization in EATs. Flow cytometry showed that HFD-fed mice have a higher proportion of total ATMs than LFD-fed mice (Fig. 3, *A* and *B*). Moreover, HFD also increased the percentage of CD11c-positive M1-like macrophages and decreased those of CD206-positive M2-like macrophages (Fig. 3, *A* and *C*), which resulted in an increment in the M1/M2 ratio of ATMs (Fig. 3*D*). Remarkably, in HFD-fed mice, moderate ʟ-lactate administration blocked these changes in total populations and subpopulations of ATMs and reversed the M1/M2 ratio (Fig. 3, *A–D*). Consistent with the reversion of the M1/M2 ratio in HFD-fed mice, moderate ʟ-lactate administration also modified the mRNA levels of several characteristic macrophage markers, including total macrophage marker *F4/80*, M1-like macrophage marker *Nos2*, and M2-like macrophage marker *Arg1* (Fig. 3, *E–G*). Together, the results show that moderate ʟ-lactate administration reduces ATM contents and suppresses proinflammatory M1 polarization in EATs in HFD-fed mice.

ʟ-lactate treatment suppressed lipopolysaccharide-induced M1 polarization in BMDMs

During the development of diet-induced obesity, serum lipopolysaccharide (LPS) level increased gradually and is positively correlated to adipose tissue inflammation and insulin resistance (13). In addition, LPS treatment could induce M1 polarization in BMDMs (33), which simulated ATM proinflammatory polarization *in vivo*. Here, LPS treatment upregulated the expressions of *NOS2*, *TNF-α*, *MCP-1*, and *IL-1β* (Fig. 4, *A–D*) and elevated the fluorescence intensities of M1 macrophage surface markers CD38 and CD274 (Fig. 4, *E* and *F*). However, 5 mM or 10 mM ʟ-lactate significantly reversed the actions of LPS treatment (Fig. 4, *A–F*). These results indicated that ʟ-lactate addition directly inhibited M1 polarization in BMDMs.

AMPKα1 mediated the inhibition of ʟ-lactate on macrophage M1 polarization

To reveal the underlying mechanisms of ʟ-lactate inhibiting macrophage M1 polarization, we sorted out macrophages from mouse EAT and detected the protein and phosphorylated levels of AMPKα1 in EATs and EAT macrophages. Compared with the mice from LS group, the mice from HS group have the decreased level of AMPKα1 phosphorylation in EATs (Fig. 5*A*). However, the decline in AMPKα1 phosphorylation was significantly reversed by moderate ʟ-lactate administration in HFD-fed mice (Fig. 5*A*). And the similar reversion of AMPKα1 phosphorylation was also found in EAT macrophages from HFD-fed mice (Fig. 5*B*). The results implied that moderate ʟ-lactate administration might inhibit ATM M1 polarization through activating AMPKα1 signaling.

To confirm the involvement, AMPK agonist, 5-aminoimidazole-4-carboxamide-1-β-ᴅ-ribofuranoside (AICAR), and inhibitor compound C were introduced in LPS-stimulated BMDMs. LPS treatment resulted in a decline in AMPKα1 phosphorylated level in BMDMs (Fig. 5*C*), along with the elevations of BMDM M1 polarization (Fig. 5, *D* and *E*) and inflammation (Fig. 5*F*). AICAR addition reversed the LPS-induced alterations, and compound C could abolish the efficiencies of AICAR (Fig. 5, *C–F*). In LPS-treated BMDMs, similar to AICAR, 10 mM ʟ-lactate also elevated AMPKα1 phosphorylation (Fig. 5*C*), and compound C also abated its action on AMPKα1 phosphorylation and macrophage M1 polarization and inflammation (Fig. 5, *D–F*). Therefore, ʟ-lactate addition suppressed proinflammatory M1 polarization in BMDMs through activating the AMPKα1 signal.

ʟ-lactate suppressed proinflammatory M1 polarization in BMDMs through activating the GPR132–PKA–AMPKα1 signal

The previous report showed that ʟ-lactate could bind to the GPR132 and promote M2 polarization of RAW264.7 macrophages and BMDMs (34). Another recent study also reported that ʟ-lactate could facilitate M2 polarization of IL-4-treated BMDMs by monocarboxylic acid transporter 1 (MCT1) (35). To explore the involvement of GPR132 or MCT1 in macrophage AMPKα1 activation induced by ʟ-lactate, we first detected their expressions in mouse macrophages. Relative to LFD, HFD downregulated *GPR132* expression in EAT and EAT ATMs (Fig. 6, *A* and *B*). However, moderate ʟ-lactate administration powerfully reversed the action of HFD on
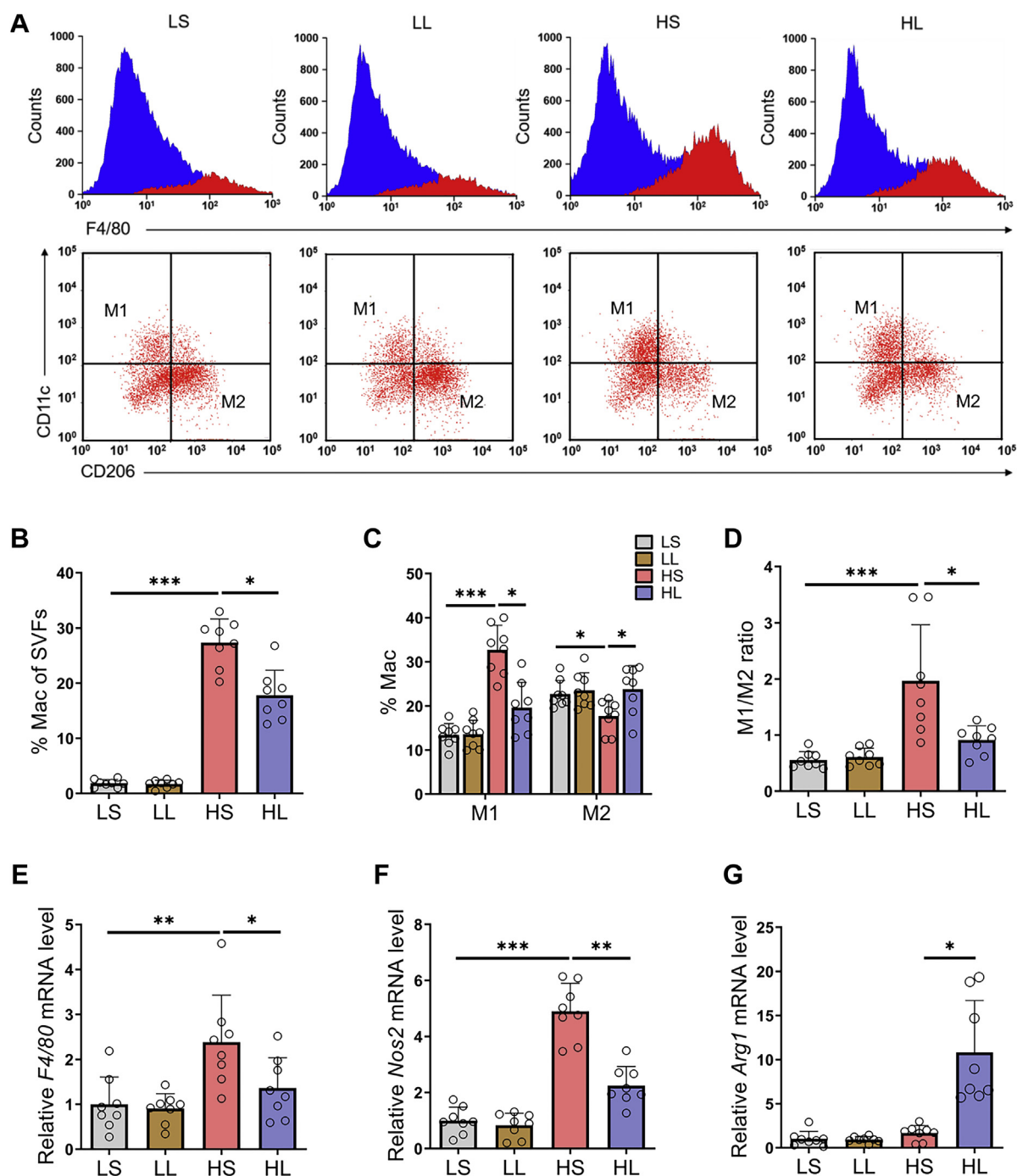
Figure 3. Moderate L-lactate administration suppressed obesity-induced ATM elevation and proinflammatory M1 polarization in EATs. *A*, using flow cytometry, F4/80$^+$ total macrophages were analyzed in SVFs from EATs, and F4/80$^+$CD11c$^+$ M1 macrophages and F4/80$^+$CD206$^+$ M2 macrophages were analyzed in F4/80$^+$ total macrophages. *B*, the total macrophage percentages in SVF cells. *C*, the M1 and M2 macrophage percentages in total macrophages. *D*, the ratio of M1 to M2 macrophages. *E–G*, the mRNA levels of total macrophage marker *F4/80* (*E*), M1 macrophage marker *Nos2* (*F*), and M2 macrophage marker *Arg1* (*G*). Data are presented as means ± SD of eight mice per group, one-way ANOVA with Mann–Whitney test; *$p < 0.05$, **$p < 0.01$, and ***$p < 0.001$. ATM, adipose tissue macrophage; EAT, epididymal adipose tissue; HL, HFD-lactate (i.p.); HS, HFD-saline (i.p.); LL, LFD-lactate (i.p.); LS, LFD-saline (i.p.); SVF, stromal vascular fraction.

GPR132 expression in EAT and EAT ATMs (Fig. 6, *A* and *B*). Unlike *GPR132* expression, both HFD and moderate L-lactate administration elevated *MCT1* expression in EAT and EAT ATMs (Fig. S5, *A* and *B*). Furthermore, *GPR132* and *MCT1* expression was examined in LPS-treated BMDMs. Similar to the action of HFD on ATM *GPR132* expression, LPS treatment also downregulated BMDM *GPR132* expression, and the

downregulation was also abated by L-lactate addition (Fig. 6C). Interestingly, either LPS or L-lactate addition also elevated *MCT1* expression in BMDMs (Fig. S5C). The results suggested that L-lactate may suppress EAT macrophage M1 polarization by GPR132, rather than by MCT1.

Next, the expression of GPR132 was detected in adipocytes and stromal vascular fraction (SVF) cells, which involve

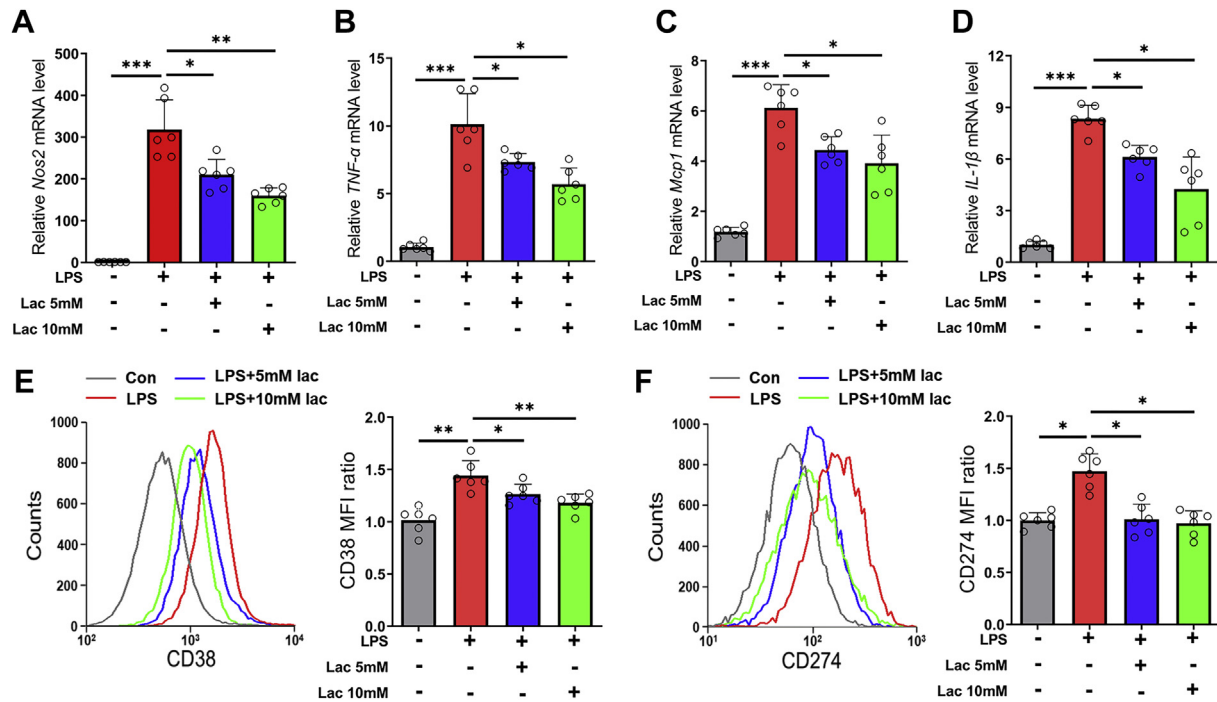**Figure 4. ʟ-lactate treatment suppressed LPS-induced M1 polarization in BMDMs.** BMDMs were treated with vehicle or ʟ-lactate (5 mM or 10 mM), and then LPS (100 ng/ml) was added. *A–D*, the mRNA levels of proinflammatory genes, including *NOS2* (*A*), *TNF-α* (*B*), *MCP1* (*C*), and *IL-1β* (*D*). *E* and *F*, flow cytometry analyses of M1 surface marker CD274 (*E*) and CD38 (*F*). Data are presented as means ± SD of six parallel samples per group, two-tailed Student's *t* test relative; *$p < 0.05$, **$p < 0.01$, and ***$p < 0.001$. BMDM, bone marrow–derived macrophage; IL-1β, interleukin 1β; Lac, ʟ-lactate; LPS, lipopolysaccharide; MCP1, monocyte chemoattractant protein 1; TNF-α, tumor necrosis factor alpha.

immune cells and adipocyte progenitors in mouse EATs. Consistent with the high expression of GPR132 in macrophages reported in the previous study (34, 36), our result also showed that GPR132 was mainly expressed in EAT SVFs (Fig. S6*A*). Furthermore, SVFs were differentiated into mature adipocytes. ʟ-lactate treatment did not affect the GPR132 expression in the mature adipocytes (Fig. S6*B*). However, in the noninduced control SVFs, 10 mM ʟ-lactate treatment significantly elevated the GPR132 expression (Fig. S6*C*). Therefore, in EATs, macrophage GPR132, but not adipocyte GPR132, was mainly in response to ʟ-lactate treatment.

It is known that the activation of GPR132 typically drives the downstream cAMP–PKA signal through Gs protein (37, 38), which promotes liver kinase B1 (LKB1) phosphorylation and subsequently activates the AMPKα1 signal in cancer cells and nerve cells (39, 40). Here, HFD also significantly reduced GPR132 expression and LKB1 phosphorylation in EATs, whereas moderate ʟ-lactate administration reversed the inhibitory actions of HFD (Fig. 6*D*). To affirm the involvements of GPR132–PKA–AMPKα1 signaling in ʟ-lactate-inhibited macrophage M1 polarization, GPR132 siRNA and PKA inhibitor H89 were introduced in LPS-stimulated BMDMs. LPS treatment reduced LKB1 and AMPKα1 phosphorylation in BMDMs, and ʟ-lactate addition reversed the effects of LPS (Fig. 6, *E* and *F*). Remarkably, the GPR132 knockdown (Figs. S7 and 6*E*) and the PKA inhibition abated the reversion of ʟ-lactate addition on LKB1 and AMPKα1 phosphorylation (Fig. 6, *E* and *F*). Consistently, the GPR132 knockdown and the PKA inhibition also reversed the repression of ʟ-lactate on the expressions of proinflammatory genes

and M1 markers in LPS-stimulated BMDMs (Fig. S8, *A–F*). Thus, ʟ-lactate suppressed proinflammatory M1 polarization in BMDMs *via* the GPR132–PKA–AMPKα1 signal.

In addition, ʟ-lactate could stimulate the secretion of TGF-β1 and TGF-β2 to induce macrophage M2 polarization (11, 41). Therefore, we investigated the expression of TGF-β1 and TGF-β2 in EATs. Relative to LFD, HFD elevated the mRNA and protein expression of TGF-β1 and reduced the protein level of TGF-β2 in EATs, but moderate ʟ-lactate administration did not alter TGF-β1 and TGF-β2 expression in EATs from either LFD-fed or HFD-fed mice (Fig. S9, *A–C*).

ʟ-lactate activated macrophage AMPKα1 signal to reduce associated adipocyte insulin resistance

As functional cells in adipose tissues, adipocytes regulate serum glucose levels through insulin signaling. The proinflammatory M1 macrophage would release various proinflammatory cytokines, such as MCP-1, TNF-α, and IL-1β, to accelerate adipose tissue inflammation and adipocyte insulin resistance (13, 14). Thus, we finally evaluated whether ʟ-lactate improves adipocyte insulin sensitivity and glucose uptake through suppressing macrophage proinflammatory polarization. Relative to those from vehicle-treated BMDMs, the conditional media from LPS-treated BMDMs increased inflammatory gene expressions (Fig. 7, *A* and *B*) and reduced AKT phosphorylation and GLUT4 translocation (Fig. 7, *C* and *D*) in 3T3-L1 adipocytes. Dramatically, ʟ-lactate addition reversed the effects of LPS-treated BMDM conditional media on adipocyte inflammation, insulin sensitivity, and glucose
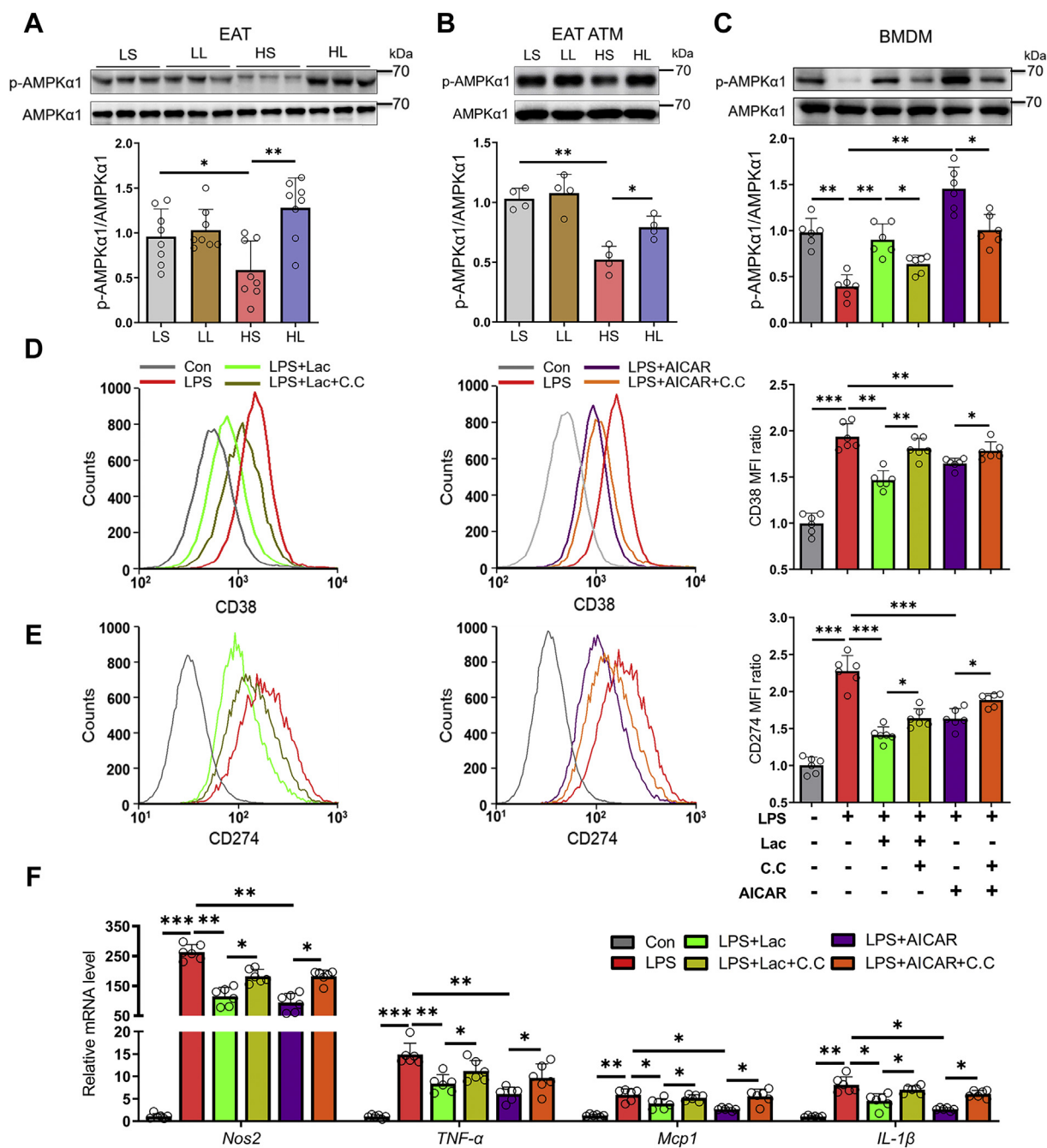
Figure 5. AMPKα1 mediated the inhibition of l-lactate on macrophage M1 polarization. The 6-week-old male mice were divided into four groups, including LS, LL, HS, and HL groups. *A*, immunoblots for phosphorylation level of AMPKα1 in EATs. *B*, immunoblots for phosphorylation level of AMPKα1 in ATMs from EATs. BMDMs were treated with vehicle, L-lactate, or AICAR, and then LPS was added. Compound C was used as an AMPK inhibitor. *C*, immunoblots for phosphorylation level of AMPKα1. *D* and *E*, flow cytometry analyses of M1 surface marker CD38 (*D*) and CD274 (*E*). *F*, the mRNA levels of proinflammatory genes. Data are presented as means ± SD of eight mice per group *in vivo*, four parallel cell samples per group in ATMs, and six parallel cell samples per group in BMDMs, one-way ANOVA with Mann–Whitney test for mice and two-tailed Student's *t* test for cell samples; *$p < 0.05$, **$p < 0.01$, and ***$p < 0.001$. AICAR, 5-aminoimidazole-4-carboxamide-1-β-D-ribofuranoside; AMPKα1, AMP-activated protein kinase alpha 1; ATM, adipose tissue macrophage; BMDM, bone marrow–derived macrophage; CC, compound C; EAT, epididymal adipose tissue; HL, HFD-lactate (i.p.); HS, HFD-saline (i.p.); Lac, L-lactate; LL, LFD-lactate (i.p.); LPS, lipopolysaccharide; LS, LFD-saline (i.p.).

uptake (Fig. 7, *A–D*), whereas compound C could abrogate the actions of L-lactate addition (Fig. 7, *A–D*).

Discussion

Lactate naturally has two optical isomers, including D-lactate and L-lactate, in which L-lactate is the dominant form

in the metabolism of mammals (42). As an endogenous metabolic intermediate, L-lactate is largely produced during exercise training (2). Moderate exercise training is considered to be an effective nonpharmacological strategy for preventing and improving obesity-associated complications, particularly type 2 diabetes (43). During moderate exercise training, plasma L-lactate levels could transiently increase to about 4 mM and
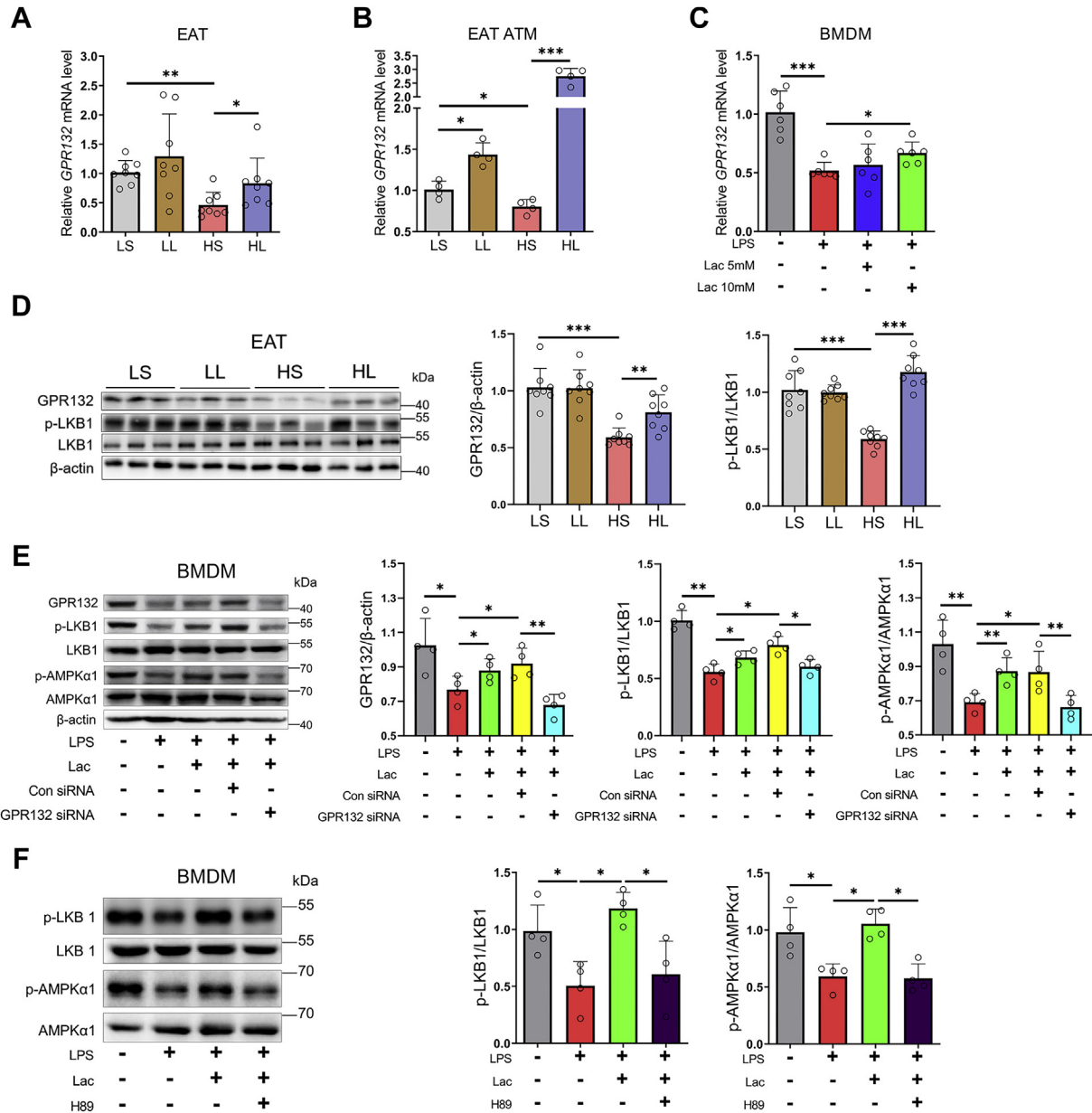
Figure 6. L-lactate activated macrophage GPR132–PKA–LKB1–AMPKα1 signal. The 6-week-old male mice were divided into four groups, including LS, LL, HS, and HL groups. *A*, the mRNA level of *GPR132* in EATs. *B*, the mRNA level of *GPR132* in ATMs from EATs. *C*, BMDMs were treated with vehicle or L-lactate (5 mM or 10 mM), and then LPS was added. The mRNA level of *GPR132* in BMDMs. *D*, immunoblots for GPR132 and phosphorylation level of LKB1 in EATs. *E*, BMDMs were treated with vehicle, L-lactate, control siRNA, or GPR132 siRNA, and then LPS was added. Immunoblots for GPR132 and phosphorylation levels of LKB1 and AMPKα1. *F*, BMDMs were treated with vehicle or L-lactate, and then LPS was added. H89 was used as a PKA inhibitor. Immunoblots for phosphorylation levels of LKB1 and AMPKα1. Data are presented as means ± SD of eight mice per group *in vivo* and four parallel cell samples per group in ATMs and BMDMs, one-way ANOVA with Mann–Whitney test for mice and two-tailed Student's *t* test for cell samples; *$p < 0.05$, **$p < 0.01$, and ***$p < 0.001$. AMPKα1, AMP-activated protein kinase alpha 1; ATM, adipose tissue macrophage; BMDM, bone marrow–derived macrophage; EAT, epididymal adipose tissue; Lac, L-lactate; LKB1, liver kinase B1; LPS, lipopolysaccharide.

return to physiological concentration in 1 to 3 h after exercise training (3, 8, 44). In this study, we adopt 800 mg/kg/day L-lactate to inject HFD-fed mice, and their plasma L-lactate concentration is elevated to 4 to 6 mM in 3 h after L-lactate injection. Thus, 800 mg/kg/day L-lactate injection is defined as a dose of moderate L-lactate administration, and 5 to 10 mM L-lactate is used as an appropriate concentration of cellular treatment. Moderate L-lactate administration obviously improves obesity-associated insulin resistance in HFD-fed mice. Meanwhile, in EATs, ATM contents and

subpopulations are modified by moderate L-lactate administration. Further mechanistic studies reveal that L-lactate treatment activates macrophage GPR132–PKA–AMPKα1 signal to suppress proinflammatory M1 polarization, finally improving adipocyte glucose homeostasis (Fig. S10).

With regarding to the effects of L-lactate on glucolipid metabolism in adipose tissues, the previous studies mainly focused on adipocytes (3, 11, 45). Carrière *et al.* (45) reported that L-lactate (5–50 mM) could promote adipocyte browning by activating PPARγ signaling. The injection of L-lactate
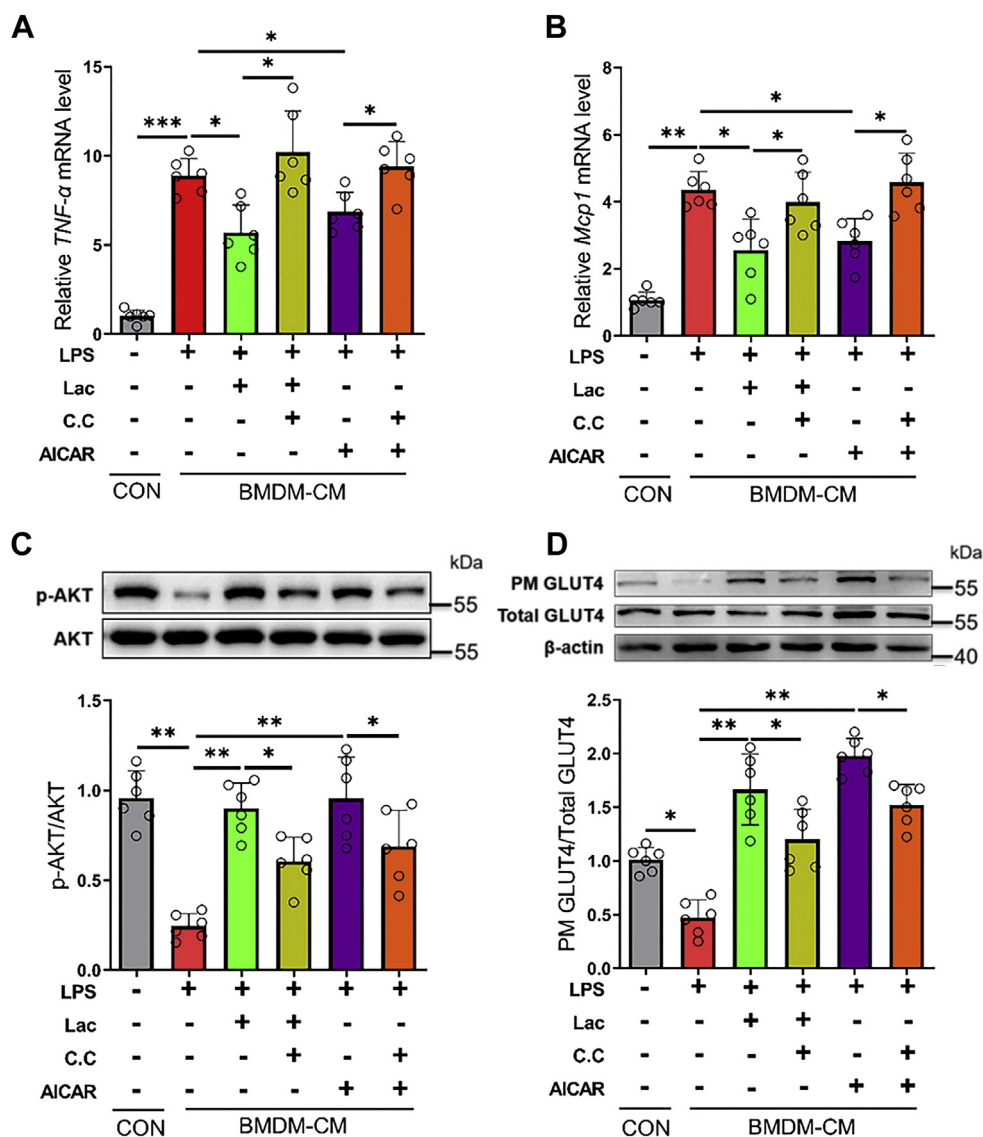
Figure 7. L-lactate activated macrophage AMPKα1 signal to reduce associated adipocyte insulin resistance. BMDMs were treated with vehicle, L-lactate, or AICAR, and then LPS was added. Compound C was used as an AMPK inhibitor. BMDMs conditional media were collected after 24 h of incubation in the fresh media. *A* and *B*, the mRNA levels of TNF-α (*A*) and MCP1 (*B*) in 3T3-L1 adipocytes. *C*, immunoblots for phosphorylated AKT (Ser473) and total AKT in 3T3-L1 adipocytes. *D*, immunoblots for plasma membrane GLUT4 and total GLUT4 in 3T3-L1 adipocytes. Data are presented as means ± SD of six parallel samples per group, two-tailed Student's *t* test; *$p < 0.05$, **$p < 0.01$, and ***$p < 0.001$. AICAR, 5-aminoimidazole-4-carboxamide-1-β-D-ribofuranoside; AMPKα1, AMP-activated protein kinase alpha 1; BMDM, bone marrow–derived macrophage; CC, compound C; CM, conditional media; Con, control; GLUT4, glucose transporter type 4; Lac, L-lactate; LPS, lipopolysaccharide; MCP1, monocyte chemoattractant protein 1; PM, plasma membrane; TNF-α, tumor necrosis factor alpha.

(about 0.002 mg/kg/day; i.p.) combined with PPARγ agonist rosiglitazone for 11 days promoted WAT thermogenesis (45). Ahmed *et al.* (3) showed that L-lactate could activate GPR81 on the adipocyte membrane and elevate the lipid storage ability of adipocytes in mice. The single-time L-lactate injection (1250 mg/kg; i.p.) strongly enhanced insulin-induced antilipolytic effects in wildtype mice rather than GPR81-deficient mice (3). A recent study by Takahashi *et al.* (11) indicated that adipokine TGF-β2 promoted adipocyte glucose uptake and attenuated adipose tissue inflammation in HFD-fed mice. L-lactate treatment (10–40 mM) increased the expression of TGF-β2 in 3T3-L1 adipocytes, and the single-time injection of L-lactate (504 mg/kg; i.p.) elevated adipokine

TGF-β2 secretion in mice (11). However, it is still unclear whether long-term moderate L-lactate injection could improve obesity-associated metabolic dysfunction in HFD-fed mice. Here, we adopted moderate L-lactate administration, a comparable dose to Ahmed *et al.* (3) and Takahashi *et al.* (11), to inject the mice for 12 weeks and found that long-term moderate L-lactate administration alleviated obesity-associated insulin resistance in HFD-fed mice (Fig. 1).

Noteworthily, a previous study by Choi *et al.* (46) showed that one-time tail vein infusion of L-lactate would impair insulin signal and induce insulin resistance in skeletal muscle. The inconsistent observations with our results should be due to different experimental aims and designs. Our study aimed to

explore the effect of long-term moderate L-lactate administration on obesity-associated insulin resistance in HFD-fed mice, while the previous study tried to assess the action of one-time L-lactate infusion on skeletal muscle insulin resistance in the rat under normal physiological conditions. The different experimental objectives lead to different experimental designs and results. First, the previous study employed the one-time tail vein infusion of L-lactate, which increased plasma L-lactate concentration to a fourfold level in 3.5 h. However, in our study, the mice were received a daily i.p. injection of L-lactate for 12 weeks, which repeatedly elevated the plasma L-lactate concentration to a twofold level in 0.5 to 1 h after L-lactate injection and then decreased to the basic level in 3 h (Fig. 1B). Second, in the previous study, insulin was preinfused for 2.5 h to activate insulin signal and then infused L-lactate and insulin for 3.5 h to assess the action of L-lactate infusion on insulin signal. In our study, the tested mice were only injected with L-lactate or saline. Third, in the previous study, the tested rats were fed with a chow diet before L-lactate infusion was performed. Yet, in our study, the tested HFD-fed mice got free access to water and food. It seems that the action of L-lactate on individual insulin sensitivity is elusive. Thus, its negative or positive effects on insulin sensitivity may greatly depend on the experimental animal kind and strain, the diet type, the animal physiological status, and the dose and duration of L-lactate treatment.

Besides adipocytes, adipose tissue also contains various SVF cells, such as adipose-derived stem/stromal cells, endothelial cells, and immune cells (32). Along with the development of obesity, the numbers and subpopulation ratios of multiple innate and adaptive immune cells dynamically altered in adipose tissues (47). In the immune cells, the proportions of macrophages, mast cells, neutrophils, dendritic cells, and CD8^{+} T cells are increased, whereas the proportions of eosinophils, Treg cells, and Th2 cells are decreased, leading to adipose tissue inflammation (13, 47). Remarkably, macrophages account for the largest proportion of these immune cells and comprise up to 40% of SVF cells in obese adipose tissue (47, 48). Meanwhile, the polarization of ATMs correlates positively with the changes in adipose tissue inflammatory status. In obese adipose tissue, the recruited ATMs polarize to F4/80^{+}CD11c^{+} proinflammatory M1 type but not F4/80^{+}CD206^{+} anti-inflammatory M2 type (14). As the major source of adipose tissue proinflammatory cytokines, M1 ATMs secrete various chemokines and cytokines, which attract more ATM and other proinflammatory immune cell recruitment, exacerbate adipose tissue inflammation, and induce local and systemic insulin resistance (47, 48). Deletion of macrophage-specific gene CCR2 would impair ATM infiltration and proinflammatory cytokine secretion, improving adipose tissue inflammation and insulin resistance (13). In addition, the regulation of other immune cells on adipose tissue inflammation mostly needs the involvement of macrophages. For instance, eosinophil-derived IL-4 and IL-13 drive ATM M2 polarization to suppress adipose tissue inflammation (16, 48). And CD8^{+} T cells promote ATM recruitment and M1 polarization to aggravate adipose tissue inflammation (48, 49).

Thus, ATMs play a central role in regulating obesity-associated adipose tissue inflammation and insulin resistance. Here, our study focused on ATMs and their subpopulations and found that moderate L-lactate treatment suppressed ATM infiltration and M1 polarization (Figs. 3 and 4).

In obese individuals, the activation of AMPKα1 inhibits several classic inflammatory signals in ATMs, such as NF-κF06BB signal and NOD-, LRR-, and pyrin domain–containing protein 3 inflammasome signal (24–26). The secretion of multiple inflammatory cytokines from ATMs, such as MCP1, TNF-α, and IL-1β, was also inhibited after AMPKα1 phosphorylation (14, 50, 51). Along with the declines in inflammatory signals and cytokines, AMPKα1 activation reduced the expressions of M1 markers, such as CD11c and NOS2, and suppressed proinflammatory polarization in ATMs (23, 24). Therefore, the AMPKα1 signal plays a critical role in ATM polarization and associated insulin resistance during diet-induced obesity. Here, our study focused on the AMPKα1 signal and found that L-lactate treatment activated the AMPKα1 signal to suppress macrophage M1 polarization (Fig. 5), which improved associated adipocyte insulin resistance (Fig. 7).

In macrophages, L-lactate could be transported into the cell by MCTs as an energy substrate or bonded to surface receptor GPR132 as a signal molecule. Previous reports about muscle regeneration and cancer indicate that L-lactate could affect macrophage polarization by cell surface receptor MCT1 and GPR132. On the one hand, L-lactate facilitates M2 polarization in IL-4-treated BMDMs by binding to MCT1 and regulating muscle regeneration (35). On the other hand, cancer cell–derived L-lactate could activate GPR132, which is highly expressed in macrophages, and result in the M0 to M2 phenotype transformation in BMDMs or RAW264.7 macrophages (34). However, it is unclear whether MCT1 or GPR132 mediated the suppression of L-lactate on ATM M1 polarization. In the context of obesity-associated inflammation, our observations suggested that L-lactate might preferentially suppress M1 polarization in macrophages through GPR132, rather than MCT1 (Figs. 6 and S5). The activation of G protein–coupled receptors would trigger the downstream cAMP–PKA signal and subsequently activate LKB1 and AMPKα1 (39, 40, 52). Correspondingly, our study also found that the activation of GPR132 would increase the PKA–LKB1–AMPKα1 signal and suppress macrophage M1 polarization (Figs. 6 and S8). In addition, since the expression of *MCT1* in ATMs and the proportion of M2 macrophage was increased in response to moderate L-lactate administration in HFD-fed mice (Figs. 3 and S5), L-lactate may also promote ATM M2 polarization *via* MCT1, a hypothesis merits further investigation.

Metabolic disorders are often accompanied by a persistent elevation in L-lactate levels. In obese individuals, blood L-lactate level is slightly increased along with the development of obesity and insulin resistance (53). However, moderate exercise training, accompanied by the transient increment of blood L-lactate concentration, can improve the common metabolic disorders (2, 7). Thus, it is of practical significance

to elucidate the paradoxical correlation between the elevation of L-lactate level and the metabolic health of organisms. In this study, moderate L-lactate administration leads to the transient increment of blood L-lactate level, similar to moderate exercise training, and recapitulates the improvements of moderate exercise training on obesity-associated insulin resistance. Although we did not well explain the aforementioned paradoxical correlation in this study, our results reveal that moderate L-lactate administration suppresses ATM M1 polarization to ameliorate insulin resistance in HFD-fed mice, suggesting a potential therapeutic and interventional approach to obesity-associated type 2 diabetes.

Experimental procedures

Animals

All male C57BL/6 mice were purchased from Vital River Laboratory Animal Technology Co Ltd at their 4 weeks old. The mice were fed on an LFD (Research Diets; D12450B containing 3.85 kcal/g and 10% fat) and maintained in a pathogen-free barrier facility with a 12 h light/12 h dark cycle. After 2 weeks of dietary and environmental adaptation, the mice were used in the following experiments. All animal experimental procedures were approved by the Ethics Committee on Animals of the Hefei University of Technology and were conducted under the guidance of international ethical standards.

Experimental design and L-lactate administration

To obtain the dose of moderate L-lactate administration, we first designed the experiment of gradient sodium L-lactate (Sigma–Aldrich) injection. At 6 weeks old, the mice were fed on an HFD (Research Diets; D12451 containing 4.73 kcal/g and 45% fat) and received L-lactate injection (i.p.) at the dose of 200, 400, 800, and 1600 mg/kg/time (twice per day), respectively. After 7 days, we weighed the mice and calculated their weight changes. The blood was collected from mouse tails, and the real-time concentrations of plasma L-lactate were detected using L-lactate assay kit (Sigma–Aldrich).

When the dose of moderate L-lactate administration was affirmed at 800 mg/kg/day, another independent study was designed to assess the effect of moderate L-lactate administration on diet-induced obesity and insulin resistance in mice. At 6 weeks old, the mice were randomly divided into four groups: (1) LS group (n = 8), fed on LFD and received saline injection (twice per day; i.p.); (2) LL group (n = 8), fed on LFD and received L-lactate injection (400 mg/kg/time; twice per day; i.p.); (3) HS group (n = 8), fed on HFD and received saline injection (twice per day; i.p.); and (4) HL group (n = 8), fed on HFD and received L-lactate injection (400 mg/kg/time; twice per day; i.p.). And then, the mouse weight and food intake were monitored each week. After 12 weeks, mouse lean and fat masses were first determined using body composition analyzer (Bruker). Glucose tolerance tests, insulin tolerance tests, and body temperature detection were conducted as the previous description (29, 54). Subsequently, mice were fed in the combined indirect calorimetry system (TSE Systems GmbH)

for 2 days. VO_2 (oxygen consumption), VCO_2 (CO_2 production), and respiratory exchange ratio were monitored in the next 24 h. Finally, the mice were sacrificed by exposure to CO_2. Their sera and tissues were harvested and stored at –80 °C. The serum pH value was detected by the blood-gas analyzer (Beckman Coulter). And the serum lipid level was detected by the biochemical analyzer (Beckman Coulter).

H&E staining

Tissues were fixed, dehydrated, embedded, and sliced at a thickness of 5 μm. The sections were subsequently deparaffinized, rehydrated, and stained with hematoxylin and eosin. Five random fields from each section were photographed, and adipocyte average diameters were measured by Image-Pro Plus, version 6.0 (Media Cybernetics).

Total RNA isolation and quantitative real-time PCR

Total RNA was isolated from the tissues or cells using RNAiso Plus reagent (Takara) and was reverse transcribed to complementary DNA by reverse transcription kit (Takara) according to the manufacturer's protocol. Quantitative real-time PCR was conducted with SYBR Premix Ex Taq II (Takara) on a real-time fluorescent quantitative PCR analyzer (Bio-Rad). All primer sequences are presented in Table S1.

Protein extraction and Western blot analysis

The tissues and cells were lysed in radio-immunoprecipitation assay lysis buffer with PMSF (Sangon) and phosphatase inhibitor complex (Sangon). The protein concentration was detected with the bicinchoninic acid assay kit (Sangon). Moreover, the membrane protein extraction kit (Sangon) was used to obtain plasma membrane protein. All protein samples were loaded on SDS-polyacrylamide gel electrophoresis and were tested by immunoblot as described previously (29). Immunoblot data were quantified by Image Quant TL 7.0 software (GE Healthcare) and were expressed as the ratio of the target protein to the corresponding reference protein. In mouse studies, eight samples per animal group were tested and quantified. In cell studies, four or six samples per cellular group were tested and quantified. Antibodies are exhibited in Table S2.

Flow cytometry and cell sorting of ATMs

SVFs were isolated from EATs as described (55). And then, the SVFs were stained with the antibody cocktail containing F4/80-APC, CD11c-PE, and CD206-FITC (Table S2). The M1 and M2 macrophages were identified, and the total macrophages were sorted by flow cytometer MoFlo XDP (Beckman Coulter). Data were analyzed using Summit 5.2 (Beckman Coulter). Flow cytometry antibodies are listed in Table S2.

BMDM culture and treatment

Bone marrows were isolated from the femurs of C57BL/6 mice. The cells were cultured in Dulbecco's modified Eagle's medium (DMEM; Gibco) containing 20% fetal bovine serum

(Gibco) and 30% L929 conditional medium for 7 days to differentiate into BMDMs as the previous description (56). To examine the action of ʟ-lactate treatment on macrophage polarization *in vitro*, BMDMs were treated with ʟ-lactate (5 mM or 10 mM) for 24 h. And then, LPS (Sigma–Aldrich; 100 ng/ml) was used to promote M1 polarization of BMDMs as previous reports (29, 33).

To explore the involvement of the PKA–AMPKα1 signal, BMDMs were first treated with AMPK inhibitor compound C (Sigma–Aldrich; 1 μM) or PKA inhibitor H89 (Sigma–Aldrich; 30 μM) for 1 h. Subsequently, AMPK agonist AICAR (Sigma–Aldrich; 0.5 mM) or ʟ-lactate (10 mM) was added. After 24 h, BMDMs were stimulated by LPS (100 ng/ml) and finally harvested as previously reported (29, 33).

BMDM siRNA transfection

The siRNAs against GPR132 and the scrambled siRNA as control were purchased from Sangon Biotech. The siRNA sequences against GPR132 were 5′-CCACAGAGCUUUCAAA CACAUUTdTdT-3′ (sense) and 5′-AUGUGUUUGAAA GCUCUGUGGTTdTdT-3′ (antisense). The negative control siRNA sequences were 5′-UUCUCCGAACGUGUCACGU TTdTdT-3′ (sense) and 5′-ACGUGACACGUUCGGAGAA TTdTdT-3′ (antisense). The siRNAs were transfected into BMDMs using Lipofectamine 3000 (Invitrogen) following the manufacturer's protocol. After 12 h, 10 mM ʟ-lactate was added to treat BMDMs for 24 h. Then, BMDMs were stimulated by LPS (100 ng/ml) and finally harvested as previously reported (29, 33).

BMDM conditioned media collection and 3T3-L1 adipocyte treatment

According to the method of Ceppo *et al.* (57), we prepared a series of BMDM conditional media. Briefly, BMDMs were treated with vehicle, ʟ-lactate (10 mM), and AICAR (0.5 mM), respectively. And then, the cells were stimulated with LPS (100 ng/ml) for 3 h and incubated in the fresh media for 24 h. Finally, the BMDM conditional media were collected.

3T3-L1 preadipocytes were purchased from the Cell Culture Center of Peking Union Medical College. The cells were cultured in DMEM (Gibco) containing 10% fetal bovine serum (Gibco) and differentiated into mature adipocytes as described previously (29). The adipocytes were cultured in BMDM conditional media for 24 h and followed by the stimulation of insulin (1 nM) for 7 min.

Primary adipocyte induction

The isolated SVF cells were cultured in DMEM (Gibco) containing 10% fetal bovine serum (Gibco). For adipogenesis, the confluent cells were cultured in the induction medium (DMEM supplemented with 850 nM insulin, 0.5 mM iso-butylmethylxanthine, 1 μM dexamethasone, and 5 μM rosi-glitazone) for 2 days. Then, the cells were maintained in DMEM supplemented with insulin and rosiglitazone for another 6 days to induce primary adipocytes.

Statistical analysis

All data were given as mean ± SD. In mouse assays, one-way ANOVA with Mann–Whitney tests was used. In cell assays, two-tailed Student's *t* tests were used. GraphPad Prism 9 (GraphPad Software, Inc) was used as statistical software, and $p < 0.05$ was considered statistically significant.

Data availability

The datasets used and/or analyzed during the current study are available from the corresponding author on reasonable request.

References

1. Hui, S., Ghergurovich, J. M., Morscher, R. J., Jang, C., Teng, X., Lu, W., Esparza, L. A., Reya, T., Le, Z., Yanxiang Guo, J., White, E., and Rabi-nowitz, J. D. (2017) Glucose feeds the TCA cycle *via* circulating lactate. *Nature* **551**, 115–118
2. Brooks, G. A. (2018) The science and translation of lactate shuttle theory. *Cell Metab.* **27**, 757–785
3. Ahmed, K., Tunaru, S., Tang, C., Muller, M., Gille, A., Sassmann, A., Hanson, J., and Offermanns, S. (2010) An autocrine lactate loop mediates

insulin-dependent inhibition of lipolysis through GPR81. *Cell Metab.* **11**, 311–319

4. Hsu, P. P., and Sabatini, D. M. (2008) Cancer cell metabolism: Warburg and beyond. *Cell* **134**, 703–707

5. Colegio, O. R., Chu, N. Q., Szabo, A. L., Chu, T., Rhebergen, A. M., Jairam, V., Cyrus, N., Brokowski, C. E., Eisenbarth, S. C., Phillips, G. M., Cline, G. W., Phillips, A. J., and Medzhitov, R. (2014) Functional polarization of tumour-associated macrophages by tumour-derived lactic acid. *Nature* **513**, 559–563

6. Ippolito, L., Morandi, A., Giannoni, E., and Chiarugi, P. (2019) Lactate: A metabolic driver in the tumour landscape. *Trends Biochem. Sci.* **44**, 153–166

7. Petridou, A., Siopi, A., and Mougios, V. (2019) Exercise in the management of obesity. *Metabolism* **92**, 163–169

8. Heden, T. D., Liu, Y., and Kanaley, J. A. (2017) Exercise timing and blood lactate concentrations in individuals with type 2 diabetes. *Appl. Physiol. Nutr. Metab.* **42**, 732–737

9. Nielsen, O. B., de Paoli, F., and Overgaard, K. (2001) Protective effects of lactic acid on force production in rat skeletal muscle. *J. Physiol.* **536**, 161–166

10. Westerblad, H., Allen, D. G., and Lännergren, J. (2002) Muscle fatigue: Lactic acid or inorganic phosphate the major cause? *News Physiol. Sci.* **17**, 17–21

11. Takahashi, H., Alves, C. R. R., Stanford, K. I., Middelbeek, R. J. W., Pasquale, N., Ryan, R. E., Xue, R., Sakaguchi, M., Lynes, M. D., So, K., Mul, J. D., Lee, M. Y., Balan, E., Pan, H., Dreyfuss, J. M., *et al.* (2019) TGF-beta2 is an exercise-induced adipokine that regulates glucose and fatty acid metabolism. *Nat. Metab.* **1**, 291–303

12. Harms, M., and Seale, P. (2013) Brown and beige fat: Development, function and therapeutic potential. *Nat. Med.* **19**, 1252–1263

13. Gregor, M. F., and Hotamisligil, G. S. (2011) Inflammatory mechanisms in obesity. *Annu. Rev. Immunol.* **29**, 415–445

14. Johnson, A. M., and Olefsky, J. M. (2013) The origins and drivers of insulin resistance. *Cell* **152**, 673–684

15. Weisberg, S. P., McCann, D., Desai, M., Rosenbaum, M., Leibel, R. L., and Ferrante, A. W., Jr. (2003) Obesity is associated with macrophage accumulation in adipose tissue. *J. Clin. Invest.* **112**, 1796–1808

16. Qiu, Y., Nguyen, K. D., Odegaard, J. I., Cui, X., Tian, X., Locksley, R. M., Palmiter, R. D., and Chawla, A. (2014) Eosinophils and type 2 cytokine signaling in macrophages orchestrate development of functional beige fat. *Cell* **157**, 1292–1308

17. Luan, B., Goodarzi, M. O., Phillips, N. G., Guo, X., Chen, Y. D., Yao, J., Allison, M., Rotter, J. I., Shaw, R., and Montminy, M. (2014) Leptin-mediated increases in catecholamine signaling reduce adipose tissue inflammation *via* activation of macrophage HDAC4. *Cell Metab.* **19**, 1058–1065

18. Chaurasia, B., Kaddai, V. A., Lancaster, G. I., Henstridge, D. C., Sriram, S., Galam, D. L., Gopalan, V., Prakash, K. N., Velan, S. S., Bulchand, S., Tsong, T. J., Wang, M., Siddique, M. M., Yuguang, G., Sigmundsson, K., *et al.* (2016) Adipocyte ceramides regulate subcutaneous adipose browning, inflammation, and metabolism. *Cell Metab.* **24**, 820–834

19. Ren, W., Xia, Y., Chen, S., Wu, G., Bazer, F. W., Zhou, B., Tan, B., Zhu, G., Deng, J., and Yin, Y. (2019) Glutamine metabolism in macrophages: A novel target for obesity/type 2 diabetes. *Adv. Nutr.* **10**, 321–330

20. Keiran, N., Ceperuelo-Mallafré, V., Calvo, E., Hernández-Alvarez, M. I., Ejarque, M., Núñez-Roa, C., Horrillo, D., Maymó-Masip, E., Rodríguez, M. M., Fradera, R., de la Rosa, J. V., Jorba, R., Megia, A., Zorzano, A., Medina-Gómez, G., *et al.* (2019) SUCNR1 controls an anti-inflammatory program in macrophages to regulate the metabolic response to obesity. *Nat. Immunol.* **20**, 581–592

21. Day, E. A., Ford, R. J., and Steinberg, G. R. (2017) AMPK as a therapeutic target for treating metabolic diseases. *Trends Endocrinol. Metab.* **28**, 545–560

22. Zhang, B. B., Zhou, G., and Li, C. (2009) Ampk: An emerging drug target for diabetes and the metabolic syndrome. *Cell Metab.* **9**, 407–416

23. Sag, D., Carling, D., Stout, R. D., and Suttles, J. (2008) Adenosine 5'-monophosphate-activated protein kinase promotes macrophage polarization to an anti-inflammatory functional phenotype. *J. Immunol.* **181**, 8633–8641

24. Leiherer, A., Mundlein, A., and Drexel, H. (2013) Phytochemicals and their impact on adipose tissue inflammation and diabetes. *Vascul. Pharmacol.* **58**, 3–20

25. Chiang, C. F., Chao, T. T., Su, Y. F., Hsu, C. C., Chien, C. Y., Chiu, K. C., Shiah, S. G., Lee, C. H., Liu, S. Y., and Shieh, Y. S. (2017) Metformin-treated cancer cells modulate macrophage polarization through AMPK-NF-κB signaling. *Oncotarget* **8**, 20706–20718

26. Zhou, H. F., Yan, H., Hu, Y., Springer, L. E., Yang, X., Wickline, S. A., Pan, D., Lanza, G. M., and Pham, C. T. (2014) Fumagillin prodrug nanotherapy suppresses macrophage inflammatory response *via* endothelial nitric oxide. *ACS Nano.* **8**, 7305–7317

27. Carneiro, L., Asrih, M., Repond, C., Sempoux, C., Stehle, J. C., Leloup, C., Jornayvaz, F. R., and Pellerin, L. (2017) AMPK activation caused by reduced liver lactate metabolism protects against hepatic steatosis in MCT1 haploinsufficient mice. *Mol. Metab.* **6**, 1625–1633

28. Kim, N., Nam, M., Kang, M. S., Lee, J. O., Lee, Y. W., Hwang, G.-S., and Kim, H. S. (2017) Piperine regulates UCP1 through the AMPK pathway by generating intracellular lactate production in muscle cells. *Sci. Rep.* **7**, 41066

29. Dong, J., Zhang, X., Zhang, L., Bian, H. X., Xu, N., Bao, B., and Liu, J. (2014) Quercetin reduces obesity-associated ATM infiltration and inflammation in mice: A mechanism including AMPKalpha1/SIRT1. *J. Lipid Res.* **55**, 363–374

30. Bogan, J. S. (2012) Regulation of glucose transporter translocation in health and diabetes. *Annu. Rev. Biochem.* **81**, 507–532

31. Kraut, J. A., and Madias, N. E. (2014) Lactic acidosis. *N. Engl. J. Med.* **371**, 2309–2319

32. Rosen, E. D., and Spiegelman, B. M. (2014) What we talk about when we talk about fat. *Cell* **156**, 20–44

33. Kratz, M., Coats, Brittney R., Hisert, Katherine B., Hagman, D., Mutskov, V., Peris, E., Schoenfelt, Kelly Q., Kuzma, Jessica N., Larson, I., Billing, Peter S., Landerholm, Robert W., Crouthamel, M., Gozal, D., Hwang, S., Singh, P. K., *et al.* (2014) Metabolic dysfunction drives a mechanistically distinct proinflammatory phenotype in adipose tissue macrophages. *Cell Metab.* **20**, 614–625

34. Chen, P., Zuo, H., Xiong, H., Kolar, M. J., Chu, Q., Saghatelian, A., Siegwart, D. J., and Wan, Y. (2017) Gpr132 sensing of lactate mediates tumor-macrophage interplay to promote breast cancer metastasis. *Proc. Natl. Acad. Sci. U. S. A.* **114**, 580–585

35. Zhang, J., Muri, J., Fitzgerald, G., Gorski, T., Gianni-Barrera, R., Masschelein, E., D'Hulst, G., Gilardoni, P., Turiel, G., Fan, Z., Wang, T., Planque, M., Carmeliet, P., Pellerin, L., Wolfrum, C., *et al.* (2020) Endothelial lactate controls muscle regeneration from ischemia by inducing M2-like macrophage polarization. *Cell Metab.* **31**, 1136–1153.e7

36. Bolick, D. T., Skaflen, M. D., Johnson, L. E., Kwon, S. C., Howatt, D., Daugherty, A., Ravichandran, K. S., and Hedrick, C. C. (2009) G2A deficiency in mice promotes macrophage activation and atherosclerosis. *Circ. Res.* **104**, 318–327

37. Tao, S. C., Gao, Y. S., Zhu, H. Y., Yin, J. H., Chen, Y. X., Zhang, Y. L., Guo, S. C., and Zhang, C. Q. (2016) Decreased extracellular pH inhibits osteogenesis through proton-sensing GPR4-mediated suppression of yes-associated protein. *Sci. Rep.* **6**, 26835

38. Okajima, F. (2013) Regulation of inflammation by extracellular acidification and proton-sensing GPCRs. *Cell. Signal.* **25**, 2263–2271

39. Wu, L., Gao, L., Zhang, D., Yao, R., Huang, Z., Du, B., Wang, Z., Xiao, L., Li, P., Li, Y., Liang, C., and Zhang, Y. (2018) C1QTNF1 attenuates angiotensin II-induced cardiac hypertrophy *via* activation of the AMPKa pathway. *Free Radic. Biol. Med.* **121**, 215–230

40. Kari, S., Vasko, V. V., Priya, S., and Kirschner, L. S. (2019) PKA activates AMPK through LKB1 signaling in follicular thyroid cancer. *Front. Endocrinol. (Lausanne)* **10**, 769

41. Zhang, F., Wang, H., Wang, X., Jiang, G., Liu, H., Zhang, G., Wang, H., Fang, R., Bu, X., Cai, S., and Du, J. (2016) TGF-β induces M2-like macrophage polarization *via* SNAIL-mediated suppression of a pro-inflammatory phenotype. *Oncotarget* **7**, 52294–52306

ASBMB

42. Brooks, G. A. (2020) Lactate as a fulcrum of metabolism. *Redox Biol.* **35**, 101454

43. Carbone, S., Del Buono, M. G., Ozemek, C., and Lavie, C. J. (2019) Obesity, risk of diabetes and role of physical activity, exercise training and cardiorespiratory fitness. *Prog. Cardiovasc. Dis.* **62**, 327–333

44. Gellen, B., Messonnier, L. A., Galactéros, F., Audureau, E., Merlet, A. N., Rupp, T., Peyrot, S., Martin, C., Féasson, L., and Bartolucci, P. (2018) Moderate-intensity endurance-exercise training in patients with sickle-cell disease without severe chronic complications (EXDRE): An open-label randomised controlled trial. *Lancet Haematol.* **5**, e554–e562

45. Carrière, A., Jeanson, Y., Berger-Müller, S., André, M., Chenouard, V., Arnaud, E., Barreau, C., Walther, R., Galinier, A., Wdziekonski, B., Villageois, P., Louche, K., Collas, P., Moro, C., Dani, C., *et al.* (2014) Browning of white adipose cells by intermediate metabolites: An adaptive mechanism to alleviate redox pressure. *Diabetes* **63**, 3253–3265

46. Choi, C. S., Kim, Y. B., Lee, F. N., Zabolotny, J. M., Kahn, B. B., and Youn, J. H. (2002) Lactate induces insulin resistance in skeletal muscle by suppressing glycolysis and impairing insulin signaling. *Am. J. Physiol. Endocrinol. Metab.* **283**, E233–E240

47. Osborn, O., and Olefsky, J. M. (2012) The cellular and signaling networks linking the immune system and metabolism in disease. *Nat. Med.* **18**, 363–374

48. Lee, Y. S., Wollam, J., and Olefsky, J. M. (2018) An integrated view of immunometabolism. *Cell* **172**, 22–40

49. Nishimura, S., Manabe, I., Nagasaki, M., Eto, K., Yamashita, H., Ohsugi, M., Otsu, M., Hara, K., Ueki, K., Sugiura, S., Yoshimura, K., Kadowaki, T., and Nagai, R. (2009) CD8+ effector T cells contribute to macrophage recruitment and adipose tissue inflammation in obesity. *Nat. Med.* **15**, 914–920

50. Sanchez-Lopez, E., Zhong, Z., Stubelius, A., Sweeney, S. R., Booshehri, L. M., Antonucci, L., Liu-Bryan, R., Lodi, A., Terkeltaub, R., Lacal, J. C., Murphy, A. N., Hoffman, H. M., Tiziani, S., Guma, M., and Karin, M. (2019) Choline uptake and metabolism modulate macrophage IL-1β and IL-18 production. *Cell Metab.* **29**, 1350–1362.e7

51. Ruderman, N. B., Carling, D., Prentki, M., and Cacicedo, J. M. (2013) AMPK, insulin resistance, and the metabolic syndrome. *J. Clin. Invest.* **123**, 2764–2772

52. Huang, Y., Zhu, X., Chen, K., Lang, H., Zhang, Y., Hou, P., Ran, L., Zhou, M., Zheng, J., Yi, L., Mi, M., and Zhang, Q. (2019) Resveratrol prevents sarcopenic obesity by reversing mitochondrial dysfunction and oxidative stress *via* the PKA/LKB1/AMPK pathway. *Aging (Albany NY)* **11**, 2217–2240

53. DiGirolamo, M., Newby, F. D., and Lovejoy, J. (1992) Lactate production in adipose tissue: A regulated function with extra-adipose implications. *FASEB J.* **6**, 2405–2412

54. Zhang, X., Zhang, Q. X., Wang, X., Zhang, L., Qu, W., Bao, B., Liu, C. A., and Liu, J. (2016) Dietary luteolin activates browning and thermogenesis in mice through an AMPK/PGC1alpha pathway-mediated mechanism. *Int. J. Obes. (Lond.)* **40**, 1841–1849

55. Bao, B., Chen, Y. G., Zhang, L., Na Xu, Y. L., Wang, X., Liu, J., and Qu, W. (2013) Momordica charantia (Bitter Melon) reduces obesity-associated macrophage and mast cell infiltration as well as inflammatory cytokine expression in adipose tissues. *PLoS One* **8**, e84075

56. Ying, W., Cheruku, P. S., Bazer, F. W., Safe, S. H., and Zhou, B. (2013) Investigation of macrophage polarization using bone marrow derived macrophages. *J. Vis. Exp.* **76**, 50323

57. Ceppo, F., Berthou, F., Jager, J., Dumas, K., Cormont, M., and Tanti, J. F. (2014) Implication of the Tpl2 kinase in inflammatory changes and insulin resistance induced by the interaction between adipocytes and macrophages. *Endocrinology* **155**, 951–964